iJRASET
International Journal For Research in
Applied Science and Engineering Technology

INTERNATIONAL JOURNAL FOR RESEARCH

IN APPLIED SCIENCE & ENGINEERING TECHNOLOGY

Volume: 6 **Issue:** IV **Month of publication:** April 2018

DOI: http://doi.org/10.22214/ijraset.2018.4341

International Journal for Research in Applied Science & Engineering Technology (IJRASET)
ISSN: 2321-9653; IC Value: 45.98; SJ Impact Factor: 6.887
Volume 6 Issue IV, April 2018- Available at www.ijraset.com

Effect of Concentration of Cadmium Acetate and Thiourea on CDS Thin Films and their Characterization

R. Murugesan[1], S. Sivakumar[2], K. Karthik[3], P. Anandan[1], M. Haris[4]
[1]*Department of Physics, Thiru Kolanjiappar Government Arts College, Vriddhachalam – 606001, India*
[1, 2]*Department of Physics, Government Arts College, Salem – 636 007, India*
[3] *School of Physics, Bharathidasan University, Tiruchirappalli – 620 024, India*
[4]*Department of Physics, Karunya Institute of Technology and Sciences, Coimbatore – 641114, India*

Abstract: Cadmium Sulphide (CdS) thin films have been coated on glass substrate at 400°C by spray pyrolysis (SP) technique using different precursor concentration (0.025M, 0.05M,0.1M,0.15M and 0.2M). CdS thin films were characterized by various techniques such as X-ray diffraction, SEM and optical studies. X-ray diffraction measurements show that CdS thin films belong to the cubic crystal structure with preferential orientation along (1 1 1) direction. The surface morphology of the thin films was analysed by scanning electron microscopy (SEM). The optical energy band gap of thin films is between 2.43 – 2.16 eV. The luminescence spectrum shows a strong green emission peak at 518 nm for 0.025M, 519 nm for 0.05M, 521 nm for 0.1M, 525 nm for 0.15M and 517 nm for 0.2M.

Keywords: Spray pyrolysis, structural studies, optical studies.

I. INTRODUCTION

Cadmium sulphide (CdS) belongs to the II-VI compound family possessing a direct bandgap of 2.4eV and large absorption coefficient of the order of 4 x 10^{-4} cm^{-1}. The size of the particle too small comparable to the wavelength of the electron makes the quantum confinement effect and hence CdS thin films might possess unique physico-chemical properties with relation to bulk CdS material. A decrease in the confining dimension also makes energy levels discrete extends up the bandgap and hence increase in the energy of the bandgap. The study on CdS is most interesting because it has large potential applications such as gas sensors, photo-detectors, solar cells, piezo-electric transducers, light emitting diodes, transparent UV protection films, biological systems (drug delivery, bio sensing and bio-imaging) etc. [1-2]. CdS thin films have been deposited by various methods such as thermal evaporation [3], sputtering [4], spray pyrolysis [5], electro deposition [6], chemical bath deposition [7], SILAR method [8] and pulsed laser deposition [9]. The spray pyrolysis technique is more advantageous when compared with other methods. It is simple, basic set-up is not expensive and flexible for process modifications and it is used for the preparation of a large number of semiconducting and insulating thin films [10]. The morphological properties of the semiconductor oxide are influenced by the film thickness, deposition technique, incorporation of dopant and concentration of the precursor solution, among other factors [11]. For example, rough surfaces of Ga-doped ZnO thin films and smooth surfaces of Al-doped ZnO thin films were obtained using the spray pyrolysis technique. Though there are many reports on doping including Ni [12], Mn [13], Co [14], Al [16], Cr [15], In [17], Sn [18], B [19], Mg [20], Er [21], etc. into CdS, the number of works on Ba, Co and Fe-doped and co-doped CdS thin film is scarce. In view of the enormous applications of CdS films in various technologies, it has been proposed to prepare CdS films by spray pyrolysis method and characterize the films. Hence, in order to identify the suitable concentration of precursor material for the preparation of CdS thin films having good adherence on the substrate, various molar concentrations of cadmium acetate and thiourea were added to prepare the solution. The prepared thin films were tested for its morphology and other functional properties like optical absorption and photoluminescence.

II. PREPARATION OF THIN FILMS

Spray pyrolysis method mainly consists of spraying solution on the heated substrate. For the thin film preparation, different precursor concentrations (0.025M, 0.05M, 0.1M, 0.15M and 0.2M) of cadmium acetate with equimolar concentration of thiourea were dissolved in 20 ml of double distilled water. Well cleaned glass substrates were placed on the heater and the distance between the tip of the nozzle and surface of the substrate was maintained at 18 cm. A constant flow rate of 3 ml/min was maintained for all the samples to be deposited on substrates maintained at 400°C. Before supplying the compressed air, the heater was allowed to heat the substrate to attain the required temperature. When compressed air along with the precursor solution was passed through the nozzle at constant pressure, finely formed aerosol descend to reach the reactor zone where the film was deposited on the heated substrate to produce CdS thin films. The precursor molar concentrations of 0.025M, 0.05M, 0.1M, 0.15M and 0.2M have been named as PC1, PC2, PC3, PC4 and PC5, respectively.

III.RESULT AND DISCUSSION

A. X-ray diffraction analysis

Figure 1 shows the X-ray diffraction patterns for different precursor CdS thin films prepared on glass substrates at 400°C. X-ray diffraction peaks are observed at 26.5°, 44° and 52° which corresponds to the (1 1 1), (2 2 0) and (3 1 1) planes, respectively. The diffraction patterns were compared with JCPDS Card No. 65-2887 and confirmed the formation of thin films. The obtained diffraction peaks correspond to the cubic structure of CdS showing a polycrystalline nature. Figure 2 shows the XRD patterns of (111) peak of CdS thin films deposited on glass substrates using different precursor concentrations. It shows that the full width at half-maximum of the (1 1 1) CdS peaks increases with the increase in the different precursor concentrations. It also shows that the intensity of the (1 1 1) CdS peaks decreases with the increase in the precursor concentration, indicating that the crystallite size of the deposited particles decreased with the increase in precursor concentration. Nucleation and the growth of nuclei compete with each other in the initial stage of thin film deposition. The generation reaction rate will be high in the case of high precursor concentration and the rate of nucleation exceeds that of the growth of nuclei, while, in the case of low precursor concentration, which leads to the predominance of rate of growth of nuclei. As the individual nuclei grow, their diameters become equal to the average distance between the nucleation sites and form a continuous film. Thus, the grain size in the films that are deposited at high precursor concentration is smaller than that in the films deposited at low precursor concentration. No significant structural change of the thin films was detected by XRD analysis. Figure 3 shows the XRD patterns of (220) and (311) peak of CdS thin films deposited on glass substrates using different precursor concentrations.

Table1 Structural parameters of CdS thin films prepared by different concentration.

Sample name	2θ (degree)	FWHM (degree)	Planes	Crystallite size D (nm)	Dislocation density ($x10^{16}$ lines/m^2)	Stacking fault (Å)
PC 1	26.50	1.136	1 1 1	7.18	1.9397	0.010344
	43.82	1.375	2 2 0	6.23	2.5803	0.009577
	51.74	2.297	3 1 1	3.84	6.7724	0.014569
PC 2	26.45	2.863	1 1 1	2.85	12.3090	0.026079
	43.91	1.754	2 2 0	4.88	4.1933	0.012199
	51.88	2.127	3 1 1	4.15	5.7985	0.013468
PC 3	26.31	7.432	1 1 1	1.10	82.996	0.067875
	43.80	1.702	2 2 0	5.03	3.9514	0.011853
	51.93	1.880	3 1 1	4.70	4.5267	0.011896
PC 4	26.43	3.390	1 1 1	2.41	17.267	0.030898
	43.86	1.884	2 2 0	4.55	4.8404	0.013112
	51.85	1.760	3 1 1	5.02	3.9700	0.011146
PC 5	26.24	3.749	1 1 1	2.18	21.128	0.034294
	43.74	1.940	2 2 0	4.41	5.1377	0.013523
	51.45	1.892	3 1 1	4.66	4.6065	0.01204

The crystallite size of the sample was determined using the Scherrer's formula [22],

$$D = K\lambda / \beta \cos\theta \qquad (1)$$

where, 'D' is the crystallite size, 'λ' is the wavelength, 'β' is the full width at half maximum of diffraction peak measured in radians, θ is the Bragg's angle.

Dislocations are the imperfections in a crystal and associate with the mis-registry of the lattice in one part of the crystal with respect to another part. Unlike vacancies and interstitial atoms, dislocations are not equilibrium imperfections. In fact, the growth mechanism involving dislocations is a matter of importance. The dislocation densities of thin films are given by the Williamson and Hall relation .

$$\delta = n / D^2 \quad (\text{lines/m}^2) \qquad (2)$$

where, ‘δ’ is dislocation density, ‘n’ is a factor which equals unity, giving minimum dislocation density.

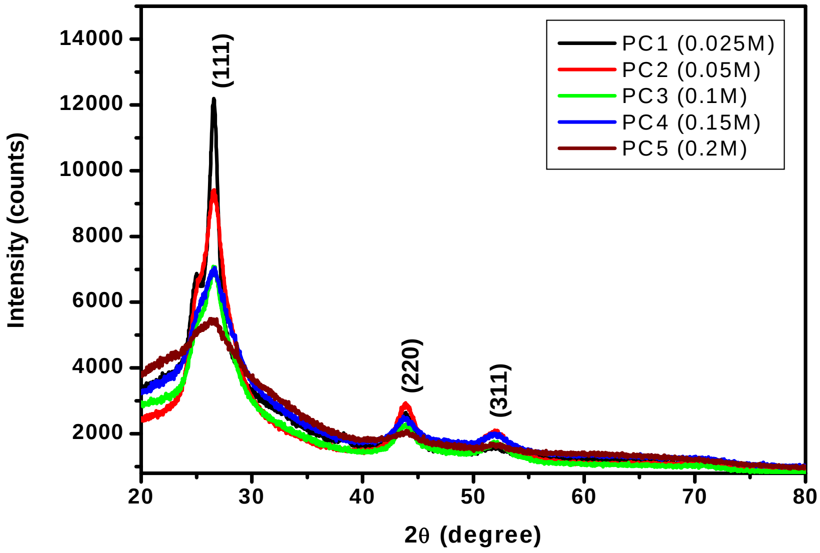

Fig. 1. XRD patterns of CdS thin films prepared with various precursor concentrations

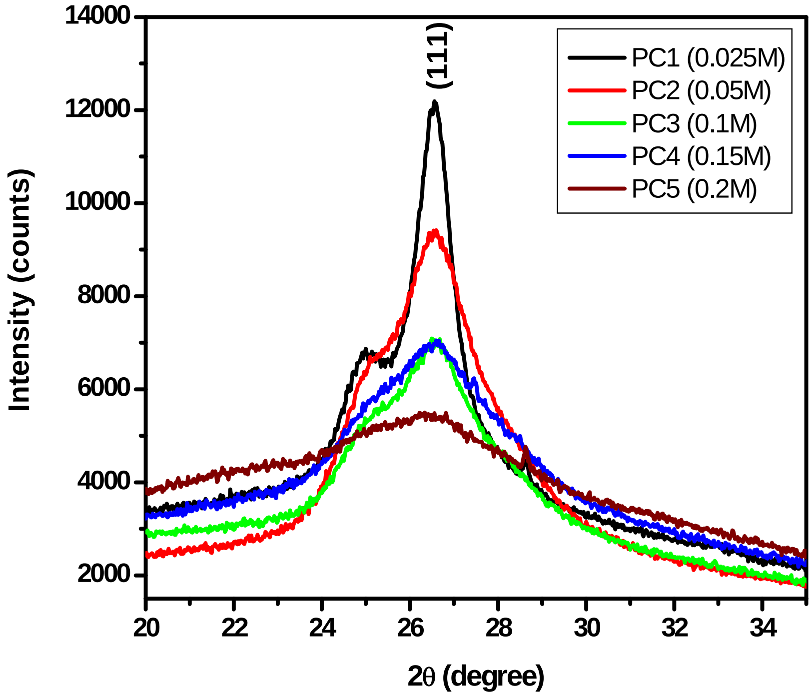

Fig. 2. Comparison of (111) plane diffraction peaks of CdS thin films prepared with various precursor concentrations

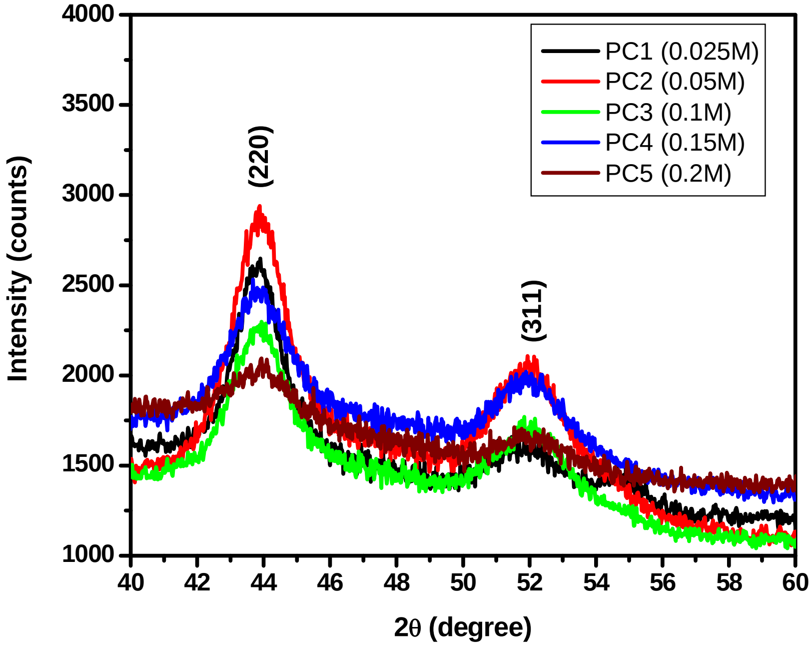

Fig. 3. Comparison of diffraction peaks related to (220) and (311) planes of CdS thin films prepared with various precursor concentrations

The stacking faults probability (α) is the fraction of layers undergoing stacking sequence faults in a given crystal and therefore, one fault is expected to be observed in 1/α layer. The existence of stacking faults gives rise to a shift in a peak position of different reflection planes with respect to ideal position of fault free sample. The relation between stacking faults probability (α) with peak shift in terms of β is given by

$$\alpha = \left[\frac{2\pi^2}{45(3\tan\theta)^{1/2}}\right] \beta \ (\text{Å}) \qquad (3)$$

where α is the stacking fault and β is FWHM.

It is observed that the dislocation density (δ) is indirectly proportional to crystallite size (D). The crystallite size, dislocation density and stacking fault values are presented in Table 1. XRD studies showed that, PC1 thin film has good crystallinity, less dislocation density and low stacking fault. The average dislocation density and stacking fault values were found to decrease with increasing precursor concentrations. The small value of dislocation density confirms that the spray pyrolysis is an effective technique to deposit good quality poly crystalline CdS thin films.

B. Morphological and Elemental Analysis

The surface morphology of the prepared CdS thin films was observed through SEM with EDS analysis (Fig. 4 and 5). Images showed that the morphology of the deposited CdS thin films was significantly affected by the variation of concentrations (PC1, PC2, PC3, PC4 and PC5). The surface morphologies of the thin films with different concentrations of the precursor (PC1-PC5) are shown in Figures 4 (a-e). As can be seen, the thin film deposited with 0.025 M precursor concentration reveals that CdS matter starts to grow on the substrate but it possesses large numbers of micro pores (Fig. 4a). At 0.05 M precursor concentration, thin films continue to grow and exhibit lesser numbers of micro pores on the surface, when compared with the previous case of the CdS thin film as seen in Figure 4(b). With an increased precursor concentration of 0.1 M, the substrate becomes well covered with significantly reduced defects along the entire surface of the substrate as seen in Figure 4(c). Beyond 0.1 M of precursor concentration, at 0.15M concentration, the thin film was observed to be peeled off from the substrate as shown in Figure 4(d). This may be related to the nonhomogeneous distribution of atoms in CdS matrix and this situation has been very often seen in the sprayed samples [23,25]. Moreover, for the case of 0.2 M the area of peeled off region is observed to be greater (Fig. 4e), which may due to the increased thickness of the films with the concentration. In this study, it can be clearly observed that the grain size of the surface increases with the film thickness, and there is a non-uniform grain size distribution on the surface. Changes in the film thickness and concentration of solution play important roles in the size of the grain. From all these figures, the effect of the film thickness on the grain size can be clearly seen. Hence, it can be inferred that the grains show an increase in size with increasing film thickness.

EDAX spectra also have been recorded during the SEM imaging technique and are shown in Fig. 5. It is observed from the Fig. 5 (a-e) that the films contain cadmium and sulphur elements predominantly. This confirms the formation of CdS thin films. However, in the case of lower precursor concentration until 0.1M, the peak related to silicon pronounced very weakly and above which, well pronounced silicon peak has been observed due to the exposure of the substrate. This has been neatly observed in the SEM images. From this study, it is clearly understood that the suitable concentration for well textured film is 0.1M.

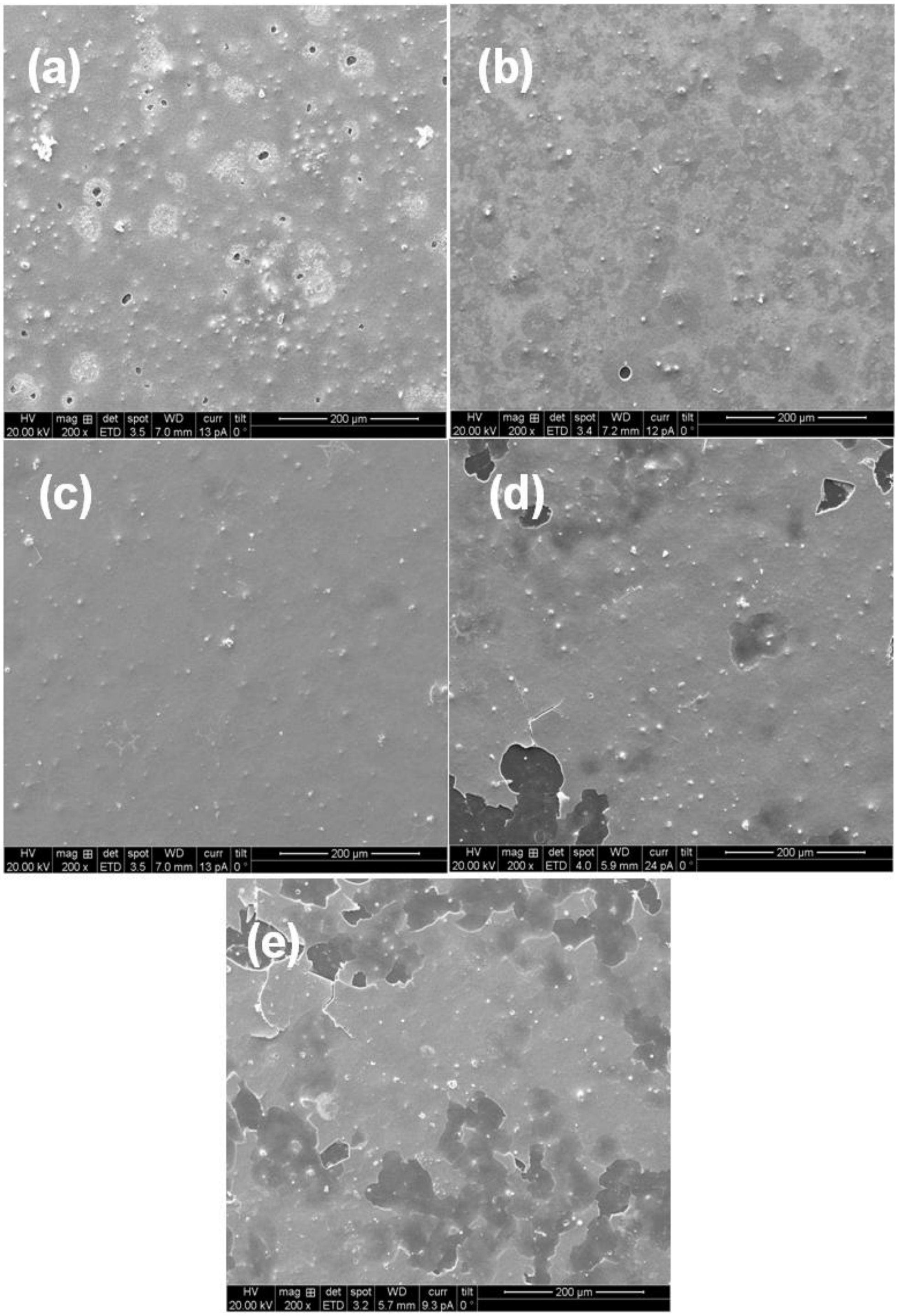

Fig. 4. SEM images of CdS thin films prepared with various precursor concentrations (PC 1 to PC 5)

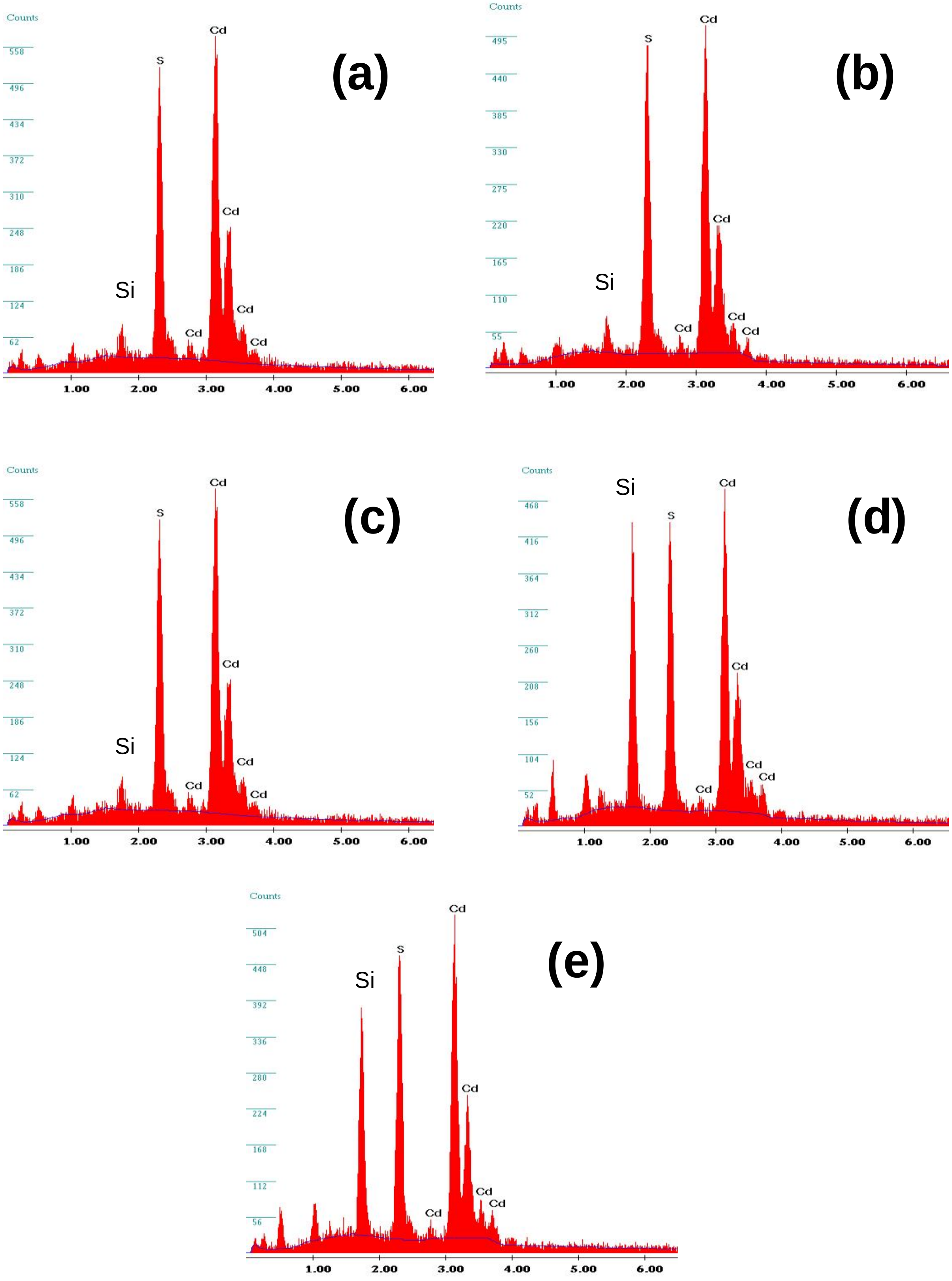

Fig. 5. EDAX spectra of CdS thin films prepared with various precursor concentrations (PC 1 to PC 5)

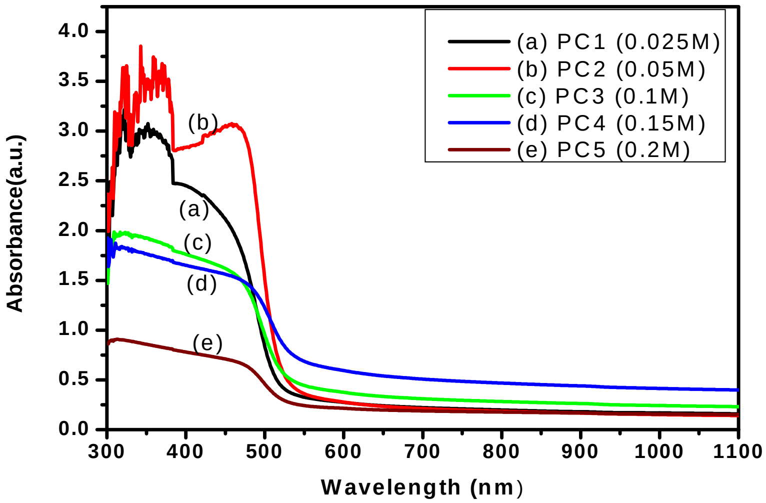

Fig. 6. Optical absorbance spectra of CdS thin films for various concentrations

C. Optical Analysis

The absorption spectra of CdS thin films for various concentrations are shown in Fig. 6. All the samples exhibit a sharp falling at the absorption edge which is an indication of a good crystallinity. The band gap values of the samples are determined using the Tauc's plot analysis [24,26]. All thin films prepared for these investigations have been found to have the absorbance edge near 540 nm in the entire visible and NIR region. The cut off wavelengths have been observed to be lesser than 540 nm and have sharp absorption edge for PC1, PC2 and even for PC3. However, the absorbance has been much reduced for the samples above 0.1M concentrations below 540 nm.

The optical band gap values have been calculated using the fundamental absorption, which corresponds to electron excitation from the valence band to the conduction band. The relation between absorption coefficient α and incident photon energy (hν) are given by the equation

$$(\alpha h\nu) = A(h\nu - E_g)^n \qquad (4)$$

where, A is a constant, E_g is the bandgap of the material and the exponent n depends on the type of transition.

Tauc plots between $(\alpha h\nu)^2$ and energy have been plotted and the linear portions of the graphs were extrapolated to meet the energy axis as shown from Fig. 7, from which the energy band gap of the respective thin films have been determined. It has been observed that, depending on different concentration of the films, the direct band gap values are varied and determined as 2.43 eV (PC 1), 2.42 eV (PC2), 2.31 eV (PC 3), 2.16 eV (PC4) and 2.35 eV (PC 5).

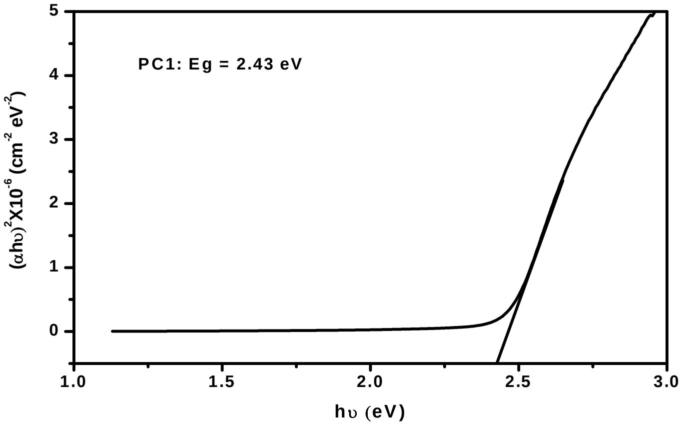

Fig.7 Optical bandgap of PC1 CdS thin film

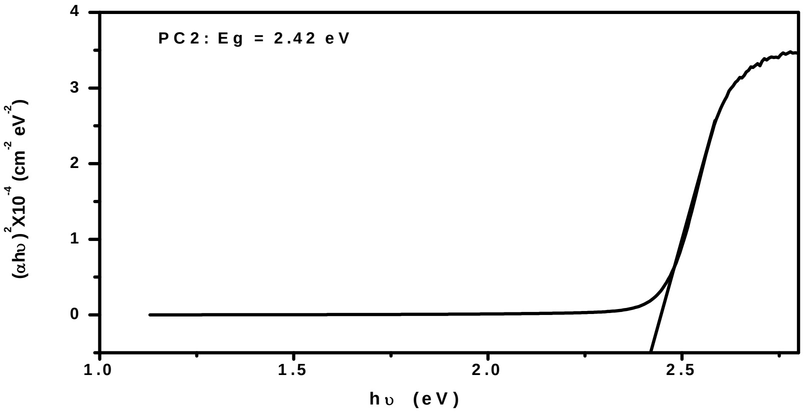

Fig.8 Optical bandgap of PC2 CdS thin film

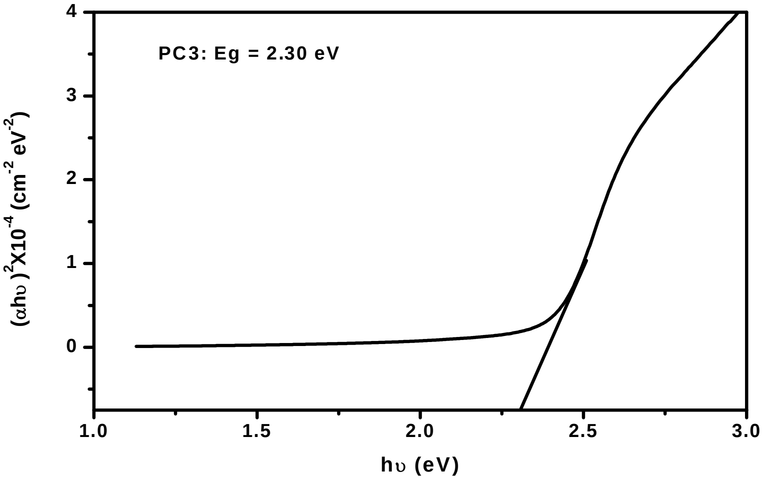

Fig. 9 Optical bandgap of PC3 CdS thin film

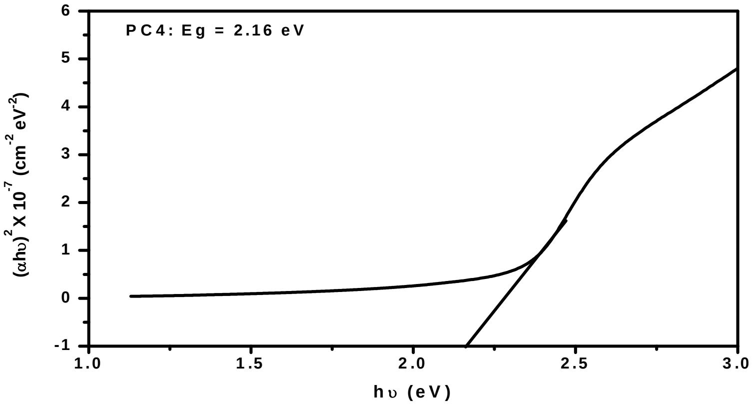

Fig. 10 Optical bandgap of PC4 CdS thin film

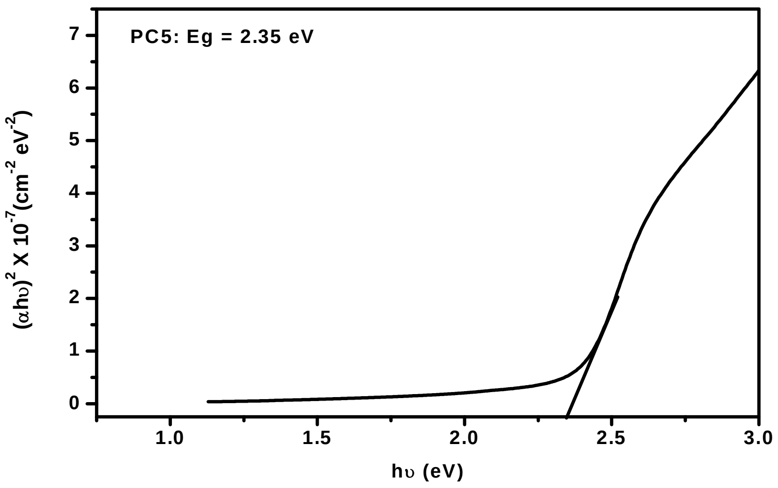

Fig. 11 Optical bandgap of PC5 CdS thin film

D. Photoluminescence Analysis

Prepared thin films have been subjected to photoluminescence study and the spectra recorded for the CdS thin films are shown in Fig. 12. Xenon lamp source at 370 nm as an exciton wavelength has been used. The luminescence originates from the recombination of surface states. In the spectra, the respective peaks at 518 nm (PC 1), 519 nm (PC 2), 521 nm (PC 3), 525 nm (PC 4) and 517 nm (PC 5) correspond to green emission of near band edge excitonic peak. The emission peaks at 518, 519, 521, 525 and 517 nm represent the green emission and peaks near 615 nm represents the yellow emission. The photoluminescence spectra are found to be dependent on the molar concentration. At the lower molar concentrations (0.025 M PC1, 0.05M PC2 and 0.1M PC3), a high strength green emission (518-520 nm) has been observed.

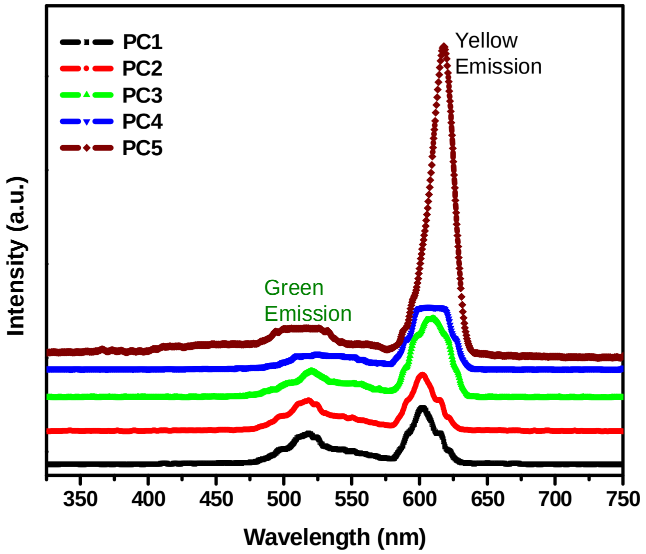

Fig.12 Photoluminescence spectrum of CdS thin films

Photoluminescence (PL) spectroscopy has also been used to determine the band gap since the most common radiative transition in the semiconductor occur between the states at the bottom of the conduction band and the top of the valence band. The intensity of PL peak prominently depends on various factors including energy level created by high defect density or impurities, film thickness and illumination time. In addition, if the film has good transparency, it might also lead to poor intensity. Though the intensity is less, it is clearly seen that there is a broad emission peak from 518 to 521 nm for PC1, PC2 and PC3. The peak at 518 nm is the near band edge emission and the band gap of pure CdS thin film is 2.39 eV. On the other hand, the peak at 518 nm has been well widened in the thin films of both PC4 and PC5 doped CdS thin films. As well, the observed widened peaks at higher molar concentrations may be due to the creation of oxygen vacancies.

IV. CONCLUSION

The CdS thin films were deposited on the glass substrate for five different molar concentrations of precursor using spray pyrolysis technique. The films were characterized by structural and optical properties. The cubic phase of CdS thin film has been observed by XRD analysis. The SEM images show that PC3 has better uniformity with minimum defects in the deposition of thin films. The optical band gap was measured to be in the range of 2.16-2.43 eV. Photoluminescence spectra show that the emissions are at 518-525 nm. The thin film of PC3 sample has finite emission property beyond which there is a broad emission in the green region. Thus, it is concluded that, PC3 is the optimum precursor concentration for the better structural and optical properties of CdS thin films.

REFERENCES

[1] V. Senthamilselvi, K. Ravichandran, K. Saravanakumar, J. Phys. Chem. Solids. 2013, 74, 65-69.
[2] Wei C W, Hou S S. Colloid Polym. Sci, 2007, 285, 1343-1349.
[3] Senthil K, Mangalaraj D, Narayandass S K, Physica B, 2001, 304, 175-180.
[4] Kim D, Park Y, Kim M, Mater. Res. Bull, 2015, 69, 78-83.
[5] Baykula M C, Balcioglu A. Microelectron. Eng, 2000, 52, 703-705.
[6] Murali K R, Kumaresan S, Prince J J. Mater. Lett, 2007, 61, 2613-2615.
[7] Gibson P N, Ozsan M E, Lincot D, Thin Solid Films, 2000, 361, 34-40.
[8] K. GowrishRao, V.K.Ashith, J. Phys. Chem. Solid. 2015, 77, 14-22.
[9] Acharya K P, Mahalingam K, Ullrich B, Thin Solid Films, 2010, 518, 1784-1787.
[10] Shashikant D. Gunjal, Yogesh B. Khollam, Sandeep A. Arote, Sandesh R. Jadkar,Pandit N. Shelke, Kakasaheb C. Mohite, Macromol. Symp. 2015, 347, 9-15.
[11] H. Gomez, A Maldonado, M. De la Olvera, D.R.Acosta, Solar Energy Mater. and Solar Cells, 2005, 87, 107-116.
[12] M. Elango, D. Nataraj, K. Prem Nazeer, M. Thamilselvan, Mater. Res. Bull. 2012, 47, 1533–1538.
[13] A. Ishizumi, K. Matsuda, T. Saiki, C.W. White, Y. Kanemitsu, Appl. Phys. Lett. 2005, 87, 133104–133106
[14] M. Muthusamy, S. Muthukumaran, M. Ashokkumar, Ceram. Int. 2014, 40, 10657–10666.
[15] S. Chandramohan, A. Kanjilal, S.N. Sarangi, S. Majumder, R. Sathyamoorthy, T.Som, J. Appl. Phys. 2009, 106, 063506–063511.
[16] K. Siva Kumar, A. Divya, P. Sreedhara Reddy, Appl. Surf. Sci. 2011, 257, 9515–9518.
[17] J. Shadia, Ikhmayies, N. Riyad, Ahmad-Bitar, J. Lumin. 2013, 142, 40–47.
[18] W. Zhou, Y. Peng, Y. Yin, Y. Zhou, Y. Zhang, D. Tang, AIP Adv. 2014, 4, 123005–123014.
[19] K.K. Challa, E. Magnone, E.-T. Kim, Mater. Lett. 2012, 85, 135–137.
[20] T. Sivaraman, A.R. Balu, V.S. Nagarethinam, Mater. Sci. Semicond. Process. 2014, 27, 915–923.
[21] J.A. Davila-Pintle, R. Lozada-Morales, M.R. Palomino-Merino, J.A.Rivera-Marquez, O. Portillo-Moreno, O. Zelaya-Angel, J. Appl. Phys. 2007, 101, 013712–013716.
[22] E.Bacaksiz, M.Tomakin, M.Altunbaş, M.Parlak, T.Çolakoğlu, Phys. B 2008, 403, 3740–3745.
[23] K. Karthik, S. Dhanuskodi, S. Prabukumar, C. Gobinath, S. Sivaramakrishnan, J. Phys. Chem. Solids 2018, 112, 106-118.
[24] K. Karthik, S. Dhanuskodi, S. Prabukumar, C. Gobinath, S. Sivaramakrishnan, J. Mater. Sci: Mater. Electron.2017, 28, 16509-16518.
[25] S. Yılmaz, ̇I. Polat, Y. Atasoy, E. Bacaksız, J. Mater. Sci: Mater. Electron. 25 (2014) 1810–1816.
[26] N. Badera, B. Godbole, S.B. Srivastava, P.N. Vishwakarma, L.S. Sharath Chandra,D. Jain, M. Gangrade, T. Shripathi, V.G. Sathe, V. Ganesan, Appl. Surf. Sci. 254 (2008) 7042–7048.

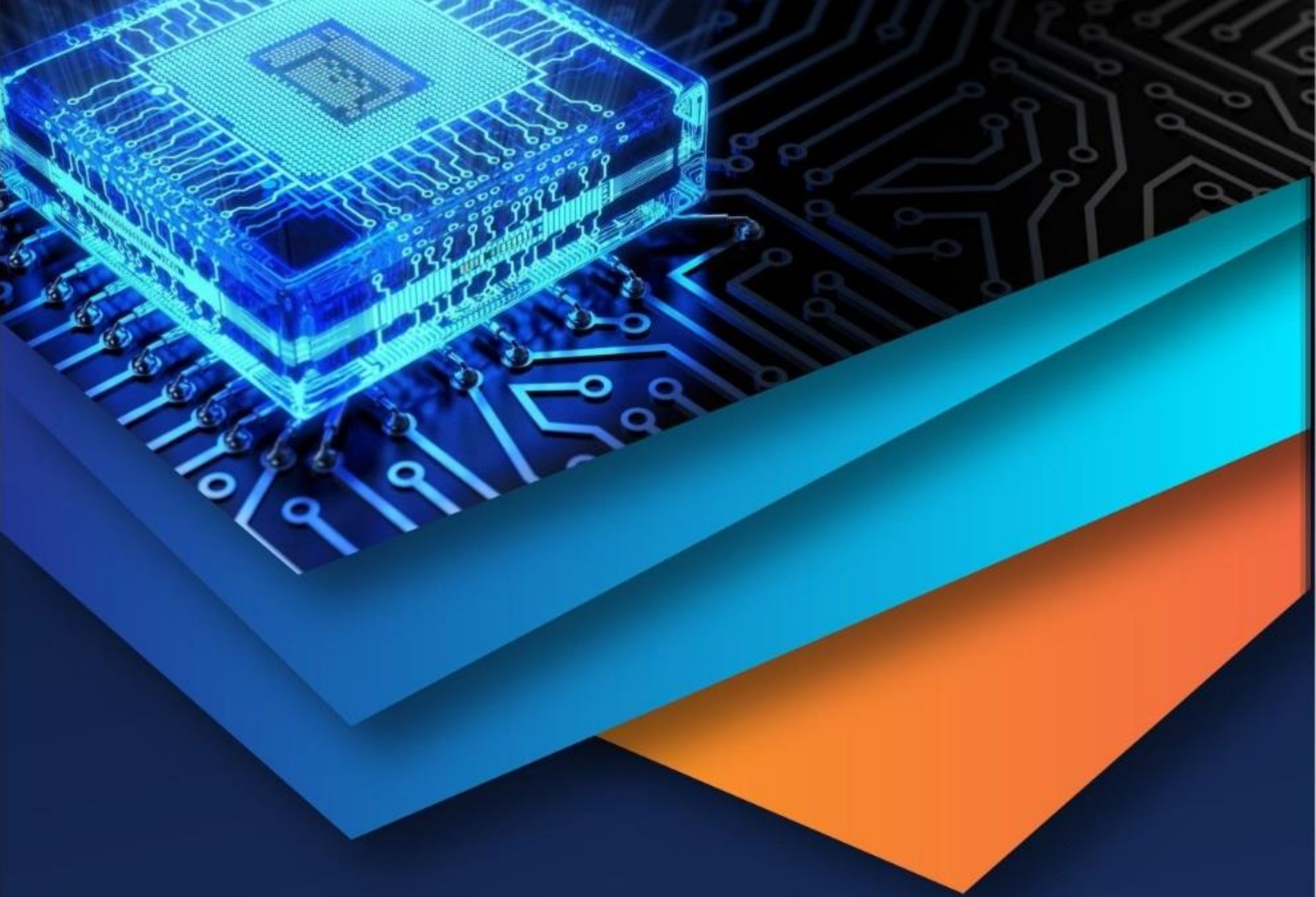

doi crossref
10.22214/IJRASET

INDEX COPERNICUS
45.98

ISRA JIF
IMPACT FACTOR:
7.129

TOGETHER WE REACH THE GOAL
IMPACT FACTOR:
7.429

ISI

INTERNATIONAL JOURNAL FOR RESEARCH

IN APPLIED SCIENCE & ENGINEERING TECHNOLOGY